The 2-silaketenyl radical (HCSiO): Ground and first excited electronic states

ARTICLE *in* JOURNAL OF MOLECULAR STRUCTURE · DECEMBER 2000

Impact Factor: 1.6 · DOI: 10.1016/S0022-2860(00)00647-5

4 AUTHORS, INCLUDING:

Shawn Brown
Carnegie Mellon University
95 PUBLICATIONS **2,988** CITATIONS
SEE PROFILE

Nicholas Petraco
City University of New York - John Jay …
28 PUBLICATIONS **251** CITATIONS
SEE PROFILE

ELSEVIER

Journal of Molecular Structure 556 (2000) 293–302

Journal of
MOLECULAR
STRUCTURE

www.elsevier.nl/locate/molstruc

The 2-silaketenyl radical (HCSiO): Ground and first excited electronic states

Y. Yamaguchi, S.T. Brown, N.D.K. Petraco, H.F. Schaefer III*

Center for Computational Quantum Chemistry, University of Georgia, Athens, GA 30602, USA

Dedicated to Professor Norman Lou Allinger

Received 9 November 1999; accepted 24 February 2000

Abstract

The ground and first excited electronic states of the 2-silaketenyl radical (HCSiO) have been studied systematically employing ab initio electronic structure theory. The ground ($\tilde{X}\,^2A''$) state of HCSiO is found to have a *trans*-planar bent structure, while the first excited ($\tilde{A}\,^2A'$) state possesses a linear equilibrium configuration. The $\tilde{X}\,^2A''$ state of HCSiO is more distorted from linearity and is more polar than the ground state of HCCO. With our most reliable level of theory, cc-pVQZ CCSD(T), the classical $\tilde{X}$–$\tilde{A}$ splitting was determined to be only 5.8 kcal/mol (0.25 eV, 2030 cm^{-1}). The ground state of HCSiO was found to be quite stable thermodynamically against the two dissociation reactions HCSiO ($\tilde{X}\,^2A''$) → H (^2S) + CSiO ($\tilde{X}\,^3\Sigma^-$) and HCSiO ($\tilde{X}\,^2A''$) → CH ($\tilde{X}\,^2\Pi$) + SiO ($\tilde{X}\,^1\Sigma^+$). HCSiO in its ground electronic state is predicted to lie 36.7 kcal/mol above the HSiCO ground state. The structural and energetic features for the two lowest-lying states of HCSiO are closer to the corresponding states of HCCO than to those of HSiCO and HSiSiO. Due to its large dipole moment and the substantial infrared (IR) intensities of some of the vibrational modes, the HCSiO radical may be suitable for microwave and IR spectroscopic investigations.

Keywords: HCSiO; HSiCO; HSiSiO; HCCO; $\tilde{X}$–$\tilde{A}$ splittings

1. Introduction

In combustion chemistry the ketenyl (HCCO) radical is known to be an important intermediate involved in the reaction [1–4]

$$HCCH + O \rightarrow HCCO + H \qquad 80 \pm 15\%, \qquad (1)$$

$$\rightarrow CH_2 + CO. \qquad (2)$$

Theoretically, the HCCO radical is a Renner–Teller molecule: the lowest $^2\Pi$ electronic state of HCCO in a linear configuration possesses one real and one imaginary vibrational frequencies along the HCC bending (or *trans* π bending) coordinates. In other words the lowest $^2\Pi$ state of HCCO is subject to a Renner–Teller interaction [5–9]. The eigenvector of the imaginary vibrational frequency leads to a *trans*-planar bent structure for the lower electronic state ($\tilde{X}\,^2A''$). The $^2A'$ component of the $^2\Pi$ state with the real bending frequency maintains the linear configuration. For the HCCO radical there are a number of experimental [10–18] and theoretical [19–25] studies that have been carried out.

In recent studies we reported the two lowest-lying states of disilaketenyl radical (HSiSiO) [26] and the 1-silaketenyl (HSiCO) radical [27]. The $\tilde{X}\,^2A''$ and

* Corresponding author. Tel.: +1-706-542-2067; fax: +1-706-542-0406.

E-mail address: hfsiii@uga.cc.uga.edu (H.F. Schaefer III).

0022-2860/00/$ - see front matter
PII: S0022-2860(00)00647-5

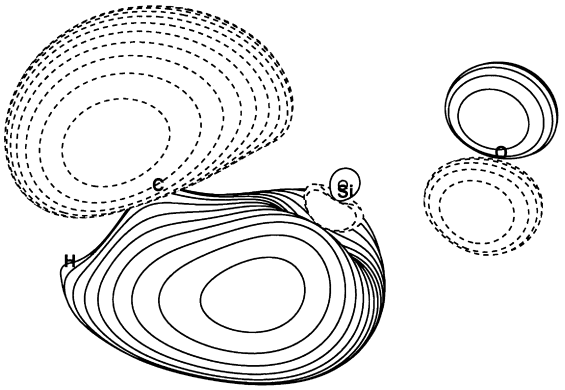

Fig. 1. The 12a′ molecular orbital of the $\tilde{X}\,^2A''$ ground state of HCSiO from the TZ2P SCF method.

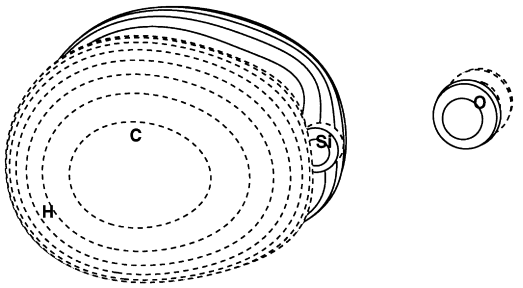

Fig. 2. The 3a″ molecular orbital of the $\tilde{X}\,^2A''$ ground state of HCSiO from the TZ2P SCF method.

$\tilde{A}^2A'$ states of the two radicals were found to be more distorted from linearity than the corresponding states of the isovalent HCCO molecule. Specifically, the HSiSi bond angle of 76° in HSiCO and the HSiC bond angle of 84° in HSiCO in their ground states are unique features of these mono- and disilaketenyl radicals. The Renner–Teller splittings of HSiSiO and HSiCO are significantly larger than the $\tilde{X}$–$\tilde{A}$ energy separation of HCCO. The present study on the HCSiO radical is a logical extension of our previous work on the ketenyl and silaketenyl radicals. To the best of our knowledge there are no experimental or theoretical studies available on the HCSiO molecule.

The structures and physical properties for the two lowest-lying states of the 2-silaketenyl radical (HCSiO), an isoelectronic isomer of HSiCO and an isovalent isomer of HCCO and HSiSiO, will be determined at the self-consistent-field (SCF) and configuration interaction with singles and double excitations (CISD) levels of theory. The energetics will be also discussed at the coupled cluster with singles and doubles (CCSD) and CCSD with perturbative triples [CCSD(T)] levels of theory. The geometries, physical properties, and energetics of HCSiO will be compared with those of the isoelectronic and/or isovalent HCCO, HSiCO, and HSiSiO molecules.

2. Electronic structure considerations

The lowest electronic state of the linear HCSiO radical has the electronic configurations:

$$[\text{core}](6\sigma)^2(7\sigma)^2(8\sigma)^2(9\sigma)^2(2\pi)^4(3\pi_i)^2(3\pi_o) \qquad 1\,^2\Pi \tag{3}$$

and

$$[\text{core}](6\sigma)^2(7\sigma)^2(8\sigma)^2(9\sigma)^2(2\pi)^4(3\pi_o)^2(3\pi_i) \qquad 1\,^2\Pi \tag{4}$$

where [core] denotes the seven core (Si:1s-,2s-,2p-like and C,O:1s-like) orbitals, and π_i and π_o stand for the in-plane and out-of-plane π molecular orbitals (MOs). The 6σ MO describes the SiO σ bonding, 7σ MO the CH σ bonding, and 8σ MO the SiC σ bonding. The 9σ MO represents a lone pair orbital on the O atom. The 2π MOs describe the SiO π bonds, while the 3π MOs comprise the SiC π bonds. At the TZ2P(f,d)-CISD level of theory this lowest $^2\Pi$ state possesses one imaginary vibrational frequency (in-plane, 261i cm^{-1}) and one real frequency (out-of-plane, 278 cm^{-1}) along the CSiO bending (or *trans* π bending) coordinates. Following the analysis of linear triatomic Renner–Teller molecules by Lee et al. [28], the $^2\Pi$ state of the HCSiO radical is classified as a type C Renner–Teller molecule. The $^2A''$ component of the $^2\Pi$ state relaxes to a non-linear equilibrium geometry:

$$[\text{core}](7a')^2(8a')^2(9a')^2(10a')^2(11a')^2(2a'')^2(12a')^2(3a'')\ \tilde{X}\,^2A'' \tag{5}$$

The 12a′ and 3a″ MOs of the $\tilde{X}\,^2A''$ state are depicted in Figs. 1 and 2, respectively. The $^2A'$ component of the lowest $^2\Pi$ state maintains the same electronic configuration as in Eq. (4).

It may be useful to discuss the instability of the SCF

reference wave functions in this section. At the linear configuration [$^2\Pi$ ($\tilde{A}\ ^2A'$)], the SCF molecular orbital (MO) Hessian (second derivatives of the SCF energy with respect to the MO rotations) [29,30] of HCSiO presents a zero eigenvalue. The eigenvector of this zero eigenvalue corresponds to a $3\pi_i$–$3\pi_o$ MO rotation, indicating that an exchange of these two MOs does not alter the SCF energy. The SCF MO Hessian for the ground state of HCSiO possesses all positive eigenvalues, showing the *stable* nature of the ground state reference wave functions. Therefore, all physical properties of the ground and first excited states may be determined without variational collapse of the reference SCF wave functions.

3. Theoretical procedures

Six triple-ζ (TZ) quality basis sets were employed in this study. The TZ basis set for Si is derived from McLean and Chandler's contraction [31] of Huzinaga's primitive Gaussian set [32]. The TZ basis sets for C, O, and H are obtained from Dunning's triple-ζ contraction [33] of Huzinaga's primitive Gaussian set [34]. The orbital exponents of the polarization functions, higher angular momentum functions, and diffuse functions were described in our previous papers [26,27]. Three correlation consistent polarized valence basis sets developed by Dunning and coworker [35,36], cc-pVDZ, cc-pVTZ, and cc-pVQZ, have been also employed. The cc-pVQZ basis set consists of 199 contracted Gaussian functions with a contraction scheme of Si (16s11p3d2f1g/6s5p3d2f1g), C and O (12s6p3d2f1g/5s4p3d2f1g), and H (6s3p2d1f/4s3p2d1f).

The self-consistent-field (SCF) method was employed to construct single configuration reference wave functions for the two lowest-lying states of the HCSiO radical. Correlation effects were included by using the single and double excitations configuration interaction (CISD), single and double excitations coupled cluster (CCSD) [37], and CCSD with perturbative triple excitations [CCSD(T)] [38] methods. The geometry optimization was performed at the SCF and CISD levels of theory. In all correlated procedures with the TZ-plus basis sets, the seven lowest-lying core orbitals (Si:1s-,2s-, and 2p-like and C,O:1s-like) were frozen and the three highest-lying virtual orbitals (Si,C,O:1s*-like) were deleted. The correlated energies with the three correlation consistent basis sets were obtained by freezing the seven core orbitals only.

In our earlier studies, the calculations without the frozen core orbital approximation using the valence TZ-plus basis sets sometimes presented anomalous behavior in predicting the geometries and energetics [26,39]. The currently available analytical derivative programs for the CCSD and CCSD(T) wave functions in our laboratory are only applicable to the cases without frozen core and deleted virtual approximations. Consequently, in the present study the CCSD and CCSD(T) methods are used only to determine the total energies at the CISD optimized geometries.

The structures of the two stationary points were optimized using analytic derivative methods [40–42]. Harmonic vibrational frequencies at the SCF level were calculated analytically, while at the CISD level of theory they were obtained by finite differences of analytic gradients. Computations were carried out using the Psi 2.0.8 program package [43] on IBM RS/6000 workstations.

4. Results and discussion

The total energies, dipole moments, harmonic vibrational frequencies, and associated infrared (IR) intensities of the two states are presented in Tables 1 ($^2\Pi$) and 2 $\tilde{X}\ ^2A''$, respectively. In Table 3 the total CISD, CCSD, and CCSD(T) energies for the $\tilde{X}\ ^2A''$, and 1 $^2\Pi$ ($\tilde{A}\ ^2A'$) states of HCSiO at the CISD optimized geometries are presented with the same TZ-plus basis set. The correlated energies with the three correlation consistent basis sets were determined at the TZ3P(2f,2d) CISD optimized geometries. Table 4 provides the relative energies of the two states at the 33 levels of theory.

4.1. Geometries

The optimized geometries for the $^2\Pi$ ($\tilde{A}\ ^2A'$) state of HCSiO are shown in Fig. 3. Given a basis set, the three bond lengths increase with inclusion of correlation effects. The equilibrium bond lengths of the diatomics CH ($\tilde{X}\ ^2\Pi$) and SiO ($\tilde{X}\ ^1\Sigma^+$) were theoretically predicted to be r_e(CH) = 1.1157 Å and r_e(SiO) = 1.5002 Å at the TZ3P(2f,2d) CISD level of theory,

Table 1
Theoretical predictions of the total energy (in hartree), dipole moment (in debye), harmonic vibrational frequencies (in cm^{-1}), and infrared intensities (in parentheses in km/mol) for the $^2\Pi$ ($\tilde{A}\ ^2A'$) state of the HCSiO molecule

Level of theory	Energy	μ_e	$\omega_1(\sigma)$ CH str.	$\omega_2(\sigma)$ CSi−SiO str.	$\omega_3(\sigma)$ CSi + SiO str.	$\omega_4(\pi_i)$ HCSi bend	$\omega_5(\pi_i)$ CSiO bend	$\omega_6(\pi_0)$ HCSi bend	$\omega_7(\pi_0)$ CSiO bend
TZ2P SCF	−402.158105	2.835	3543(75.4)	1505(219.7)	1068(0.7)	410(0.1)	213i(−)	470(16.3)	307(85.2)
TZ2P + diff SCF	−402.158822	2.889	3544(74.8)	1503(224.8)	1067(0.9)	413(0.0)	203i(−)	475(16.3)	306(84.6)
TZ3P SCF	−402.160936	2.874	3532(70.2)	1514(217.1)	1072(0.8)	414(0.0)	180i(−)	479(14.6)	303(79.1)
TZ2P(f,d) SCF	−402.163866	2.824	3535(70.6)	1508(219.3)	1069(0.6	426(0.6)	135i(−)	481(18.5)	305(87.8)
TZ2P(f,d) + diff SCF	−402.164513	2.883	3536(71.2)	1506(226.8)	1068(0.9)	428(1.4)	128i(−)	486(19.2)	304(86.1)
TZ3P(2f,2d) SCF	−402.168864	2.850	3530(67.2)	1516(216.0)	1073(0.7)	432(1.0)	114i(−)	489(16.5)	304(79.1)
TZ2P CISD	−402.550918	2.618	3477(67.5)	1427(141.7)	1011(0.8)	365(1.1)	365i(−)	396(6.2)	262(71.9)
TZ2P + diff CISD	−402.552193	2.678	3477(67.0)	1425(147.0)	1010(1.0)	364(0.9)	365i(−)	396(6.2)	260(71.5)
TZ3P CISD	−402.559061	2.644	3459(64.7)	1442(141.4)	1019(0.7)	360(1.9)	358i(−)	381(3.8)	260(67.8)
TZ2P(f,d) CISD	−402.591185	2.627	3487(67.5)	1443(144.6)	1022(0.8)	386(0.0)	261i(−)	452(15.7)	278(67.7)
TZ2P(f,d) + diff CISD	−402.592260	2.694	3487(67.9)	1441(150.9)	1021(1.1)	386(0.1)	258i(−)	455(16.3)	275(66.1)
TZ3P(2f,2d) CISD	−402.607608	2.647	3471(65.0)	1454(145.7)	1027(0.7)	388(0.0)	265i(−)	444(11.7)	276(62.9)

Table 2
Theoretical predictions of the total energy (in hartree), dipole moment (in debye), harmonic vibrational frequencies (in cm^{-1}), infrared intensities (in parentheses in km/mol), and zero-point vibrational energy (ZPVE in kcal/mol) for the $\tilde{X}\ ^2A''$ state of the *trans*-HCSiO molecule

Level of theory	Energy	μ_e	$\omega_1(a')$ CH str.	$\omega_2(a')$ CSi−SiO str.	$\omega_3(a')$ CSi + SiO str.	$\omega_4(a')$ HCSi bend	$\omega_5(a')$ CSiO bend	$\omega_6(a'')$ tors.	ZPVE
TZ2P SCF	−402.159271	3.006	3445(22.3)	1447(163.1)	973(19.8)	384(77.9)	252(79.3)	360(0.2)	9.81
TZ2P + diff SCF	−402.159990	3.041	3441(21.7)	1443(166.9)	968(20.9)	382(78.3)	252(74.5)	359(0.3)	9.79
TZ3P SCF	−402.161992	2.964	3425(20.6)	1455(161.5)	971(20.5)	383(79.3)	256(73.0)	357(0.7)	9.79
TZ2P(f,d) SCF	−402.164424	3.015	3452(28.5)	1454(167.5)	990(15.3)	388(61.6)	219(92.6)	367(0.2)	9.82
TZ2P(f,d) + diff SCF	−402.165137	3.067	3444(26.3)	1449(171.2)	981(17.5)	388(65.3)	228(81.3)	365(0.2)	9.80
TZ3P(2f,2d) SCF	−402.169366	2.970	3448(27.1)	1464(167.3)	992(15.3)	384(58.4)	222(86.1)	367(0.6)	9.83
TZ2P CISD	−402.556625	2.980	3297(4.1)	1346(90.5)	875(23.9)	520(61.5)	261(37.3)	324(0.6)	9.47
TZ2P + diff CISD	−402.558156	3.019	3291(3.9)	1342(95.0)	870(25.1)	526(61.8)	260(35.7)	325(0.5)	9.46
TZ3P CISD	−402.564809	2.889	3279(4.4)	1361(92.0)	883(24.0)	538(62.7)	265(36.5)	325(0.0)	9.51
TZ2P(f,d) CISD	−402.595021	2.989	3325(8.4)	1362(94.5)	896(19.1)	493(66.0)	264(38.7)	331(0.3)	9.54
TZ2P(f,d) + diff CISD	−402.596360	3.032	3318(7.9)	1358(99.4)	892(20.5)	504(65.0)	264(36.4)	332(0.3)	9.53
TZ3P(2f,2d) CISD	−402.611366	2.898	3321(9.2)	1378(97.8)	905(18.6)	498(66.7)	266(38.1)	332(0.0)	9.58

Table 3
Total CISD, CCSD, and CCSD(T) energies in hartree for the $\tilde{X}\ ^2A''$ and $\tilde{A}\ ^2A'$ states of HCSiO at their CISD optimized geometries with the same TZ-plus basis sets. The total energies with the three correlation consistent basis sets were determined at the TZ3P(2f,2d) CISD optimized geometries

Electronic state Level of theory	$\tilde{X}\ ^2A''$ *trans*	$^2\Pi$ ($\tilde{A}\ ^2A'$) linear
cc-pVDZ CISD	−402.459407	−402.451099
cc-pVTZ CISD	−402.598650	−402.593822
cc-pVQZ CISD	−402.639702	−402.635919
TZ2P CCSD	−402.608943	−402.599497
TZ2P + diff CCSD	−402.610812	−402.600928
TZ3P CCSD	−402.617843	−402.608359
TZ2P(f,d) CCSD	−402.651508	−402.644176
TZ2P(f,d) + diff CCSD	−402.653137	−402.645383
TZ3P(2f,2d) CCSD	−402.669121	−402.662035
cc-pVDZ CCSD	−402.505365	−402.494015
cc-pVTZ CCSD	−402.655432	−402.647308
cc-pVQZ CCSD	−402.699711	−402.692636
TZ2P CCSD(T)	−402.632829	−402.620945
TZ2P + diff CCSD(T)	−402.634916	−402.622492
TZ3P CCSD(T)	−402.642494	−402.630613
TZ2P(f,d) CCSD(T)	−402.677474	−402.667858
TZ2P(f,d) + diff CCSD(T)	−402.679290	−402.669158
TZ3P(2f,2d) CCSD(T)	−402.696327	−402.687068
cc-pVDZ CCSD(T)	−402.522927	−402.509431
cc-pVTZ CCSD(T)	−402.681791	−402.671521
cc-pVQZ CCSD(T)	−402.728597	−402.719337

while the experimental values are r_e(CH) = 1.1198 Å and r_e (SiO) = 1.5097 Å [44]. The CH bond length in HCSiO is considerably shorter than for the diatomic CH molecule, whereas the SiO bond length in HCSiO stays about the same as that for diatomic SiO.

The linear $^2\Pi$ state of HCSiO is subject to a Renner–Teller interaction, and the $^2A''$ component is stabilized to a *trans*-planar bent structure, as seen in Fig. 4. The three bond lengths for this $\tilde{X}\ ^2A''$ state increase with inclusion of correlation effects, as found for the linear $^2\Pi$ stationary point. The $12a'$ MO in Eq. (5) (depicted in Fig. 1) reflects weak Si–C π (in-plane) and C–H σ bonding character, while the $3a''$ MO in Eq. (5) (shown in Fig. 2) has strong Si–C π (out-of-plane) bonding character. The difference between the electronic configurations (4) and (5) makes the CH and SiC bond distances of the ground state longer compared to those of the $^2\Pi$ ($\tilde{A}\ ^2A'$) state. The SiO bond length remains about the same for both the $\tilde{X}\ ^2A''$ and $\tilde{A}\ ^2A'$ states. The two bond angles of the ground state considerably decrease with the treatment of correlation effects and they are quite sensitive to the basis set.

Table 4
The $\tilde{X}\ ^2A''$–$\tilde{A}\ ^2A'$ splitting for the HCSiO radical

Level of theory	ΔE kcal/mol	ΔE eV	ΔE cm^{-1}
TZ2P SCF	0.73	0.032	256
TZ2P + diff SCF	0.73	0.032	256
TZ3P SCF	0.66	0.029	232
TZ2P(f,d) SCF	0.35	0.015	122
TZ2P(f,d) + diff SCF	0.39	0.017	137
TZ3P(2f,2d) SCF	0.32	0.014	110
TZ2P CISD	3.58	0.155	1250
TZ2P + diff CISD	3.74	0.162	1310
TZ3P CISD	3.61	0.156	1260
TZ2P(f,d) CISD	2.41	0.104	842
TZ2P(f,d) + diff CISD	2.57	0.112	900
TZ3P(2f,2d) CISD	2.36	0.102	825
cc-pVDZ CISD	5.21	0.226	1820
cc-pVTZ CISD	3.03	0.131	1060
cc-pVQZ CISD	2.37	0.103	830
TZ2P CCSD	5.93	0.257	2070
TZ2P + diff CCSD	6.20	0.269	2170
TZ3P CCSD	5.95	0.258	2080
TZ2P(f,d) CCSD	4.60	0.200	1610
TZ2P(f,d) + diff CCSD	4.87	0.211	1700
TZ3P(2f,2d) CCSD	4.45	0.193	1560
cc-pVDZ CCSD	7.12	0.309	2490
cc-pVTZ CCSD	5.10	0.221	1780
cc-pVQZ CCSD	4.44	0.193	1550
TZ2P CCSD(T)	7.46	0.323	2610
TZ2P + diff CCSD(T)	7.80	0.338	2730
TZ3P CCSD(T)	7.46	0.323	2610
TZ2P(f,d) CCSD(T)	6.03	0.262	2110
TZ2P(f,d) + diff CCSD(T)	6.36	0.276	2220
TZ3P(2f,2d) CCSD(T)	5.81	0.252	2030
cc-pVDZ CCSD(T)	8.47	0.367	2960
cc-pVTZ CCSD(T)	6.44	0.279	2250
cc-pVQZ CCSD(T)	5.81	0.252	2030

4.2. Dipole moments

With the TZ3P(2f,2d) CISD method the dipole moments were predicted to be 2.90 Debye for the $\tilde{X}\ ^2A''$ state and 2.65 Debye for the $\tilde{A}\ ^2A'$ state. The theoretically predicted dipole moments generally decrease somewhat with the treatment of electron correlation and with the basis set size. According to Pauling [45], the standard electronegativities of the four relevant atoms are H(2.1), C(2.5), Si(1.8), and O(3.4). The larger difference in the electronegativities

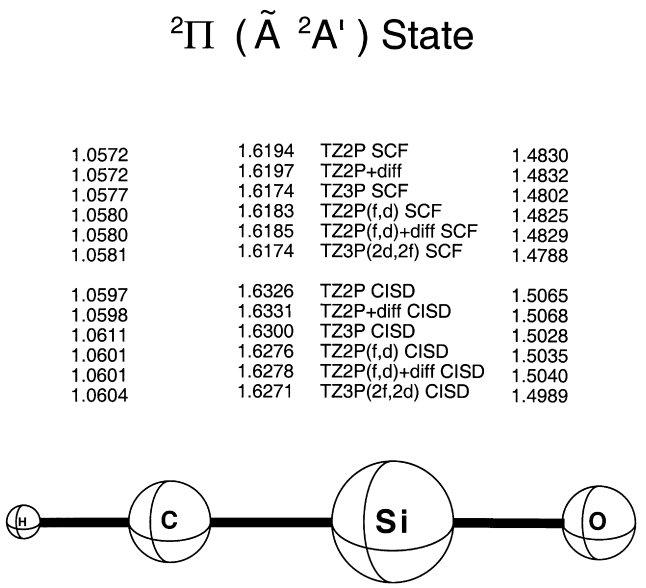

Fig. 3. Predicted geometries for the lowest $^2\Pi$ ($\tilde{A}$ $^2A'$) state of HCSiO at the twelve levels of theory. Bond lengths are in Å.

of Si–O compared to C–O may be attributed to the larger dipole moment of HCSiO than HCCO (1.59 Debye for the $\tilde{X}$ $^2A''$ state) [24]. Since the dipole moment of $\tilde{X}$ $^2A''$ state of HCSiO is predicted to be relatively large, microwave spectroscopic investigations may be feasible for this radical.

4.3. Harmonic vibrational frequencies

The three stretching (ω_1–ω_3) vibrational frequencies of the $\tilde{X}$ $^2A''$ and $\tilde{A}$ $^2A'$ states of HCSiO are predicted be smaller at the CISD level than the SCF method, probably due to the longer bond distances. Furthermore the three stretching modes of the ground state present lower frequencies than the corresponding values for the linear stationary point. The harmonic vibrational frequencies of the diatomic CH ($\tilde{X}$ $^2\Pi$) and SiO ($\tilde{X}$ $^1\Sigma^+$) molecules were theoretically determined to be ω_e (CH) = 2892 cm^{-1} and ω_e (SiO) = 1319 cm^{-1} at the TZ3P(2f,2d) CISD level of theory, while the experimental values are ω_e (CH) = 2858.5 cm^{-1} and ω_e (SiO) = 1241.6 cm^{-1}, respectively [44]. The CH stretching (ω_1) frequencies of HCSiO are significantly higher than the corresponding frequency of the diatomic CH molecule. These features are consistent with Badger's rule that a shorter bond length is associated with a higher vibrational frequency (larger force constant) [46,47]. The pure SiO stretching mode is not clearly observed in the HCSiO system, owing to a strong interaction with the CSi stretching motion. Since the HCSi and CSiO bond angles of the ground state are smaller at the CISD level of theory, the two in-plane bending motions (ω_4 and ω_5) present larger frequencies with the CISD method compared to the SCF method.

4.4. Infrared (IR) intensities

The CSi–SiO stretching (ω_2) mode shows the largest IR intensities among the six vibrational modes. This may be due to the fact that the difference in electronegativities among the four constituent atoms is the largest between the Si and O atoms. The IR intensities of the CH stretching (ω_1), CSi–SiO stretching (ω_2), and CSiO bending (ω_5) modes significantly diminish with correlation effects. IR spectroscopic studies of this molecule may be possible due to relatively large intensities of several vibrational modes.

4.5. Energetics

4.5.1. $^2A''$–$^2A'$ splitting

With the TZ3P(2f,2d) basis set, the classical $\tilde{X}$–$\tilde{A}$ splitting was predicted to be 0.32 (SCF), 2.36 (CISD),

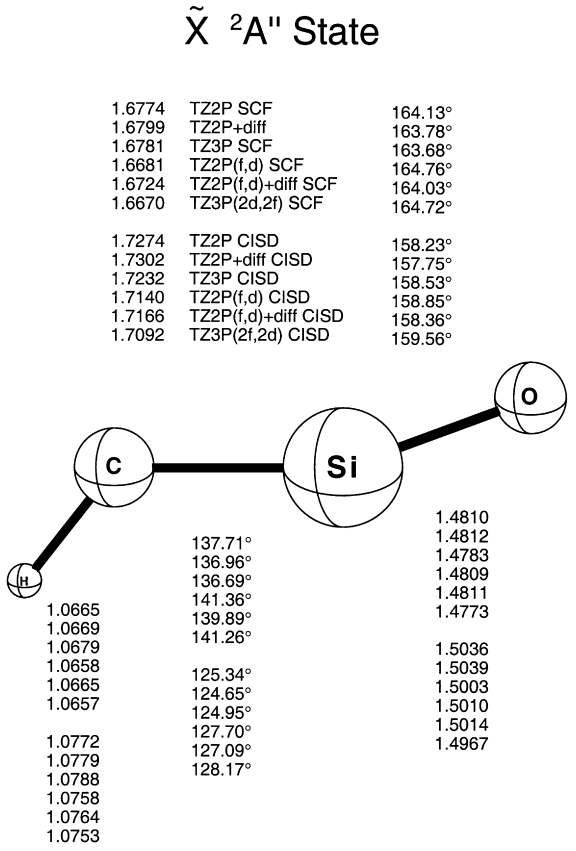

Fig. 4. Predicted geometries for the $\tilde{X}\,^2A''$ state of HCSiO at the twelve levels of theory. Bond lengths are in Å.

4.45 (CCSD), and 5.81 kcal/mol [CCSD(T)], respectively. It is seen that advanced treatments of correlation effects increase significantly this energy separation. On the other hand an increase of the basis set size generally decreases the X̃–Ã splitting. With a given correlated method, the cc-pVDZ basis set provides the largest energy separation, while the cc-pVQZ basis set presents the similar splitting as the TZ3P(2f,2d) basis set. At the most reliable level of theory, cc-pVQZ CCSD(T), the classical energy separation was determined to be 5.81 kcal/mol (0.252 eV, 2030 cm^{-1}). This energy gap is about three times larger than the corresponding value of 1.84 kcal/mol for the HCCO system [24]. It is seen in Table 4 that the X̃–Ã energy separation is convergent in terms of the basis set expansion and the level of correlation effects.

4.5.2. Dissociation energies

In order to examine the stability of the HCSiO radical the following two dissociation reactions were investigated:

$$HCSiO\ (\tilde{X}\,^2A'') \rightarrow H\ (^2S) + CSiO\ (\tilde{X}\,^3\Sigma^-) \quad (6)$$

and

$$HCSiO\ (\tilde{X}\,^2A'') \rightarrow CH\ (\tilde{X}\,^2\Pi) + SiO\ (\tilde{X}\,^1\Sigma^+) \quad (7)$$

Employing the cc-pVQZ CCSD(T) method, the total energies of HCSiO ($\tilde{X}\,^2A''$) and CSiO ($\tilde{X}\,^3\Sigma^-$) were determined to be −402.728597 (this study) and −402.066512 hartree (Ref. [48]) at their respective TZ3P(2f,2d) CISD geometries. The SCF energy of H (^2S) with the cc-pVQZ basis set is known to be −0.499946 hartree. Consequently, the dissociation energy for the reaction (6) becomes D_e = 101.7 kcal/mol (35 600 cm^{-1}). Employing the CISD zero-point vibrational energy (ZPVE) correction, the quantum mechanical dissociation energy becomes D_0 = 95.5 kcal/mol (33 400 cm^{-1}).

The cc-pVQZ CCSD(T) total energies of CH ($\tilde{X}\,^2\Pi$) and SiO ($\tilde{X}\,^1\Sigma^+$) were determined to be −38.418735 and −364.228684 hartree at their respective TZ3P(2f,2d) CISD geometries. As a result, the classical dissociation energy for the reaction (7) becomes D_e = 50.9 kcal/mol (17 800 cm^{-1}). Using the CISD ZPVE correction, the quantum mechanical dissociation energy becomes 47.4 kcal/mol (16 600 cm^{-1}). It is seen that the ground state of HCSiO is quite stable thermodynamically against the two dissociation reactions.

4.6. Comparison of HCCO, HCSiO, HSiCO, and HSiSiO

In Table 5 the structural and energetic features of the four ketenyl radicals are compared. The HCCO and HCSiO radicals are classified as type C, while the HSiCO and HSiSiO species are characterized as type D Renner–Teller molecules [28]. The XY (where X,Y = C or Si) distances of the ground state of the four ketenyl radicals are elongated by 2.85% (HCCO), 5.04% (HCSiO), 11.9%(HSiCO), and 12.8% (HSiSiO) relative to the XY bond lengths of the respective linear structures ($^2\Pi$). Since the formation of multiple bonds is most efficient at a linear configuration, it is seen that the Si atoms in ketenyl radicals

Table 5
Comparison of ketenyl and silaketenyl radicals, HXYO (X, Y: C or Si)

Physical properties	HCCO[a]	HCSiO[b]	HSiCO[c]	HSiSiO[d]
Renner–Teller type[e]	C	C	D	D
Structure				
$\tilde{X}\ ^2A''$	*trans*-bent	*trans*-bent	*trans*-bent	*trans*-bent
$\tilde{A}\ ^2A'$	linear	linear	*trans*-bent	*trans*-bent
XY distance[f]				
$1\ ^2\Pi$	1.261	1.627	1.668	2.023
$\tilde{X}\ ^2A''$	1.297	1.709	1.867	2.282
$\tilde{A}\ ^2A'$	1.261	1.627	1.740	2.115
∠XYO angle				
$\tilde{X}\ ^2A''$	169.4°	159.6°	175.0°	179.8°
$\tilde{A}\ ^2A'$	180.0°	180.0°	177.4°	174.5°
∠HXY angle				
$\tilde{X}\ ^2A''$	134.6°	128.2°	84.1°	75.6°
$\tilde{A}\ ^2A'$	180.0°	180.0°	115.7°	120.8°
Dipole moment[g]				
$1\ ^2\Pi$	2.04	2.65	2.89	4.38
$\tilde{X}\ ^2A''$	1.59	2.90	0.38	2.78
$\tilde{A}\ ^2A'$	2.04	2.65	1.52	3.54
$\tilde{X}$–$\tilde{A}$ splitting[h]	1.8_4	5.8_1	35.7	36.3
Barrier to linearity[h]				
$\tilde{X}\ ^2A''$	1.8_4	5.8_1	53.5	45.2
$\tilde{A}\ ^2A'$	–	–	17.8	8.9_3
$H(^2S) + XYO\ (\tilde{X}\ ^3\Sigma^-)$[i]				
$\tilde{X}\ ^2A''$	104.2	101.7	70.3	71.5
	(98.0)	(95.5)	(66.2)	(67.8)
$XH(\tilde{X}\ ^2\Pi) + YO(\tilde{X}\ ^1\Sigma^+)$[i]	73.8	50.9	28.7	24.5
$\tilde{X}\ ^2A''$	(68.9)	(47.4)	(25.9)	(22.8)

[a] Data from Ref. [24]. At the cc-pVTZ CCSD(T) level of theory.
[b] Geometries and dipole moments are at the TZ3P (2f,2d) CISD level of theory from this study.
[c] Data from Ref. [27]. At the TZ3P (2f,2d) CISD level of theory.
[d] Data from Ref. [26]. At the TZ3P (2f,2d) CISD level of theory.
[e] See text and Ref. [28].
[f] Bond lengths are in Å.
[g] Dipole moments are in debye.
[h] Enegetics are in kcal/mol at the cc-pVQZ CCSD(T) level of theory except HCCO [24].
[i] Dissociation energies, D_e values (D_0 values in parentheses), are in kcal/mol with the cc-pVQZ CCSD(T) method at the TZ3P(2f,2d) CISD optimized geometries. This study.

are unfavorable for the formation of the multiple bonds. For the ground state the deviation of the XYO angles from linearity is larger for HCCO and HCSiO than for HSiCO and HSiSiO. On the contrary, HXY angles are significantly smaller for HSiCO and HSiSiO relative to HCCO and HCSiO.

In his excellent article titled “Chemical Bonding in High Main Group Elements” [49], Kutzelnigg discussed the fact that the s and p valence atomic orbitals (AOs) of first row atoms are localized in roughly the same region of space, while the valence AOs of second or higher row atoms are much more extended in space. Consequently, single bonds between first row atom elements are weak and multiple bonds are strong, whereas for the higher row elements single bonds are strong and multiple bonds are weak. For the XH_n type hydrides, Kutzelnigg further stated [50] that ideal hybridization is

realized if s and p valence AOs are localized in the same region of space and hence have comparable bonding and overlapping power. This is the case only for first row atoms, and particularly for carbon. In elements of the higher rows the actual valence configurations differ considerably from the ideal hybrids. They are, in fact, somewhere between the ground configurations and the ideal valence configurations. The structural features of the four ketenyl radicals (HCCO, HCSiO, HSiCO, and HSiSiO) shown in Table 5 are quite consistent with Kutzelnigg's arguments [49,50].

The dipole moments of the $\tilde{X}\,^2A''$ state of the four ketenyl-like radicals are in the order:

$$\mu_e(\mathrm{HCSiO}) > \mu_e(\mathrm{HSiSiO}) > \mu_e(\mathrm{HCCO}) > \mu_e(\mathrm{HSiCO}) \quad (8)$$

For the ground state, the HCSiO molecule is the most polar and the HSiCO is the least polar. The dipole moments of the electronically excited $\tilde{A}\,^2A'$ states of the four ketenyl radicals are in the order:

$$\mu_e(\mathrm{HSiSiO}) > \mu_e(\mathrm{HCSiO}) > \mu_e(\mathrm{HCCO}) > \mu_e(\mathrm{HSiCO}) \quad (9)$$

For the first excited state, the HSiSiO molecule is the most polar and the HSiCO is the least polar.

The $\tilde{X}$–$\tilde{A}$ splittings of HCCO and HCSiO are almost an order of magnitude smaller compared to the energy separations of HSiCO and HSiSiO. As reflected by the HXY bond angles, the formation of the weak C···H interaction in HSiCO and Si···H interaction in HSiSiO may be attributed to the large barriers to linearity of these two radicals. The four ketenyl radicals in their ground states are quite stable against dissociation reactions of the type HXYO ($\tilde{X}\,^2A''$) → H(^2S) + XYO ($\tilde{X}\,^3\Sigma^-$). On the other hand, the HCCO and HCSiO are very stable against the dissociation reaction of the type HXYO ($\tilde{X}\,^2A''$) → XH ($\tilde{X}\,^2\Pi$) + YO ($\tilde{X}\,^1\Sigma^+$), whereas the HSiCO and HSiSiO are moderately stable against the dissociation reaction of the same type.

4.7. Energetic comparison of HSiCO, SiCOH, HCSiO, and CSiOH

In order to determine the global minimum of the four atom molecules, geometry optimizations for the SiCOH and CSiOH isomers have been carried out at the TZ2P(f,d) CISD level of theory. The ground state SiCOH radical has a planar *trans*-bent structure, whereas ground state CSiOH has planer *trans*-bent and *cis*-bent equilibrium structures. The total energies (in hartree) of these isomers are −402.598484 for *trans*-bent $\tilde{X}\,^2A''$SiCOH, −402.538216 for *trans*-bent $\tilde{X}\,^2A''$ CSiOH, and −402.537780 for *cis*-bent $\tilde{X}\,^2A''$ CSiOH, respectively. Using the total TZ2P(f,d) CISD energies (in hartree) from previous [27] and current studies of −402.659807 for *trans*-bent $\tilde{X}\,^2A''$ HSiCO and −402.595021 for *trans*-bent $\tilde{X}\,^2A''$ HCSiO, the relative energies (in kcal/mol) of the five isomers are predicted to be HSiCO (0.0) < SiCOH (38.5) < HCSiO (40.7) < *trans* CSiOH (76.3) < *cis* CSiOH (76.6). Therefore, the global minimum of this four atom system is predicted to be the HSiCO radical [27], while the HCSiO radical in the present study is found to be the third stable isomer. With the cc-pVQZ CCSD(T) method at the TZ3P(2f,2d) CISD optimized geometries, the ground state of HCSiO lies 36.7 kcal/mol (1.59 eV, 12 800 cm − 1) above the ground state of HSiCO.

5. Concluding remarks

The two lowest-lying electronic states of the 2-silaketenyl radical, HCSiO, have been studied systematically employing ab initio SCF, CISD, CCSD, and CCSD(T) levels of theory with a wide range of basis sets. The ground state of HCSiO is found to have a *trans*-planar bent structure, while the first excited state has a linear configuration. The $\tilde{X}$–$\tilde{A}$ splitting of the two states is predicted to be 5.8 kcal/mol (0.25 eV, 2 030 cm − 1). The geometrical and energetic features of the $\tilde{X}\,^2A''$ and $\tilde{A}\,^2A'$states of HCSiO are found to be similar to HCCO rather than to HSiCO or HSiSiO. Due to a relatively large dipole moment and the large IR intensities of some of the vibrational modes, microwave and infrared spectroscopic investigations are feasible for the HCSiO radical.

Acknowledgements

This research was supported by the U.S. National Science Foundation, Grant CHE-9815397.

References

[1] J. Warnatz, in: W.C. Gardiner (Ed.), Combustion Chemistry, Springer, Berlin, 1984, p. 288.
[2] J.V. Michael, A.F. Wagner, J. Phys. Chem. 94 (1990) 2453.
[3] W. Boullart, J. Peeters, J. Phys. Chem. 96 (1992) 9810.
[4] J. Peeters, I. Langhans, W. Boullart, Int. J. Chem. Kinet. 26 (1994) 869.
[5] G. Herzberg, E. Teller, Z.Phys Chem. Abt. B 21 (1933) 410.
[6] R. Renner, Z.Phys Chem. 92 (1934) 172.
[7] G. Herzberg, Molecular Spectra and Molecular Structure III. Electronic Spectra and Electronic Structure of Polyatomic Molecules, Van Nostrand, Princeton, NJ, 1966.
[8] Ch. Jungen, A.J. Merer, in: K.N. Rao (Ed.), Molecular Spectroscopy: Modern Research, 2, Academic Press, New York, 1976, p. 127.
[9] J.M. Brown, F. Jørgensen, Adv. Chem. Phys. 52 (1983) 117.
[10] S.L.N.G. Krishnamachari, R. Venkatasubramanian, Prama 23 (1984) 321.
[11] Y. Endo, E. Hirota, J. Chem. Phys. 86 (1987) 4319.
[12] K.G. Unfried, R.F. Curl, J. Mol. Spectrosc. 150 (1991) 86.
[13] K.G. Unfried, G.P. Glass, R.F. Curl, Chem. Phys. Lett. 177 (1991) 33.
[14] R. Venkatasubramanian, S.L.N.G. Krishnamachari, Indian J. Pure Appl. Phys. 29 (1991) 697.
[15] Y. Oshima, Y. Endo, J. Mol. Spectrosc. 159 (1993) 458.
[16] D.H. Mordaunt, D.L. Osborn, H. Choi, R.T. Bise, D.M. Neumark, J. Chem. Phys. 105 (1996) 6078.
[17] L.R. Brock, B. Mischler, E.A. Rohlfing, R.T. Bise, D.M. Neumark, J. Chem. Phys. 107 (1997) 665.
[18] D.L. Osborn, D.H. Mordaunt, H. Choi, R.T. Bise, D.M. Neumark, C.M. Rohlfing, J. Chem. Phys. 106 (1997) 10087.
[19] L.B. Harding, J. Phys. Chem. 85 (1981) 10.
[20] D.L. Cooper, Astrophys. J. 265 (1983) 808.
[21] J.D. Goddard, Chem. Phys. Lett. 154 (1989) 387.
[22] C.-H. Hu, H.F. Schaefer, Z. Hou, K.D. Bayes, J. Am. Chem. Soc. 115 (1993) 6904.
[23] P.G. Szalay, J.F. Stanton, R.J. Bartlett, Chem. Phys. Lett. 193 (1992) 573.
[24] P.G. Szalay, G. Fogarasi, L. Nemes, Chem. Phys. Lett. 263 (1996) 91.
[25] P.G. Szalay, J.-P. Blaudeau, J. Chem. Phys. 106 (1997) 436.
[26] S.T. Brown, Y. Yamaguchi, H.F. Schaefer, J. Chem. Phys. 111 (1999) 227.
[27] Y. Yamaguchi, N.D.K. Petraco, S.T. Brown, H.F. Schaefer, J. Chem. Phys. 112 (2000) 2168.
[28] T.J. Lee, D.J. Fox, H.F. Schaefer, R.M. Pitzer, J. Chem. Phys. 81 (1984) 356.
[29] Y. Yamaguchi, I.L. Alberts, J.D. Goddard, H.F. Schaefer, Chem. Phys. 147 (1990) 309.
[30] N.A. Burton, Y. Yamaguchi, I.L. Alberts, H.F. Schaefer, J. Chem. Phys. 147 (1990) 309.
[31] A.D. McLean, G.S. Chandler, J. Chem. Phys. 72 (1980) 5639.
[32] S. Huzinaga, Approximate Atomic Functions II, Department of Chemistry Report, University of Alberta, Edmonton, Alberta, Canada, 1971.
[33] T.H. Dunning, J. Chem. Phys. 55 (1971) 716.
[34] S. Huzinaga, J. Chem. Phys. 42 (1965) 1293.
[35] T.H. Dunning, J. Chem. Phys. 90 (1989) 1007.
[36] D.E. Woon, T.H. Dunning, J. Chem. Phys. 98 (1993) 1358.
[37] G.D. Purvis, R.J. Bartlett, J. Chem. Phys. 76 (1982) 1910.
[38] K. Raghavachari, G.W. Trucks, J.A. Pople, M. Head-Gorden, Chem. Phys. Lett. 157 (1989) 479.
[39] N.D.K. Petraco, S.T. Brown, Y. Yamaguchi, H.F. Schaefer, J. Phys. Chem. (2000) (in press).
[40] P. Pulay, Mol. Phys. 17 (1969) 197.
[41] P. Pulay, in: H.F. Schaefer (Ed.), Modern Theoretical Chemistry, 4, Plenum Press, New York, 1977, pp. 153–185.
[42] Y. Yamaguchi, Y. Osamura, J.D. Goddard, H.F. Schaefer, A New Dimension to Quantum Chemistry: Analytic Derivative Methods in Ab Initio Molecular Electronic Structure Theory, Oxford University Press, New York, 1994.
[43] C.L. Janssen, E.T. Seidl, G.E. Scuseria, T.P. Hamilton, Y. Yamaguchi, R.B. Remington, Y. Xie, G. Vacek, C.D. Sherrill, T.D. Crawford, J.T. Fermann, W.D. Allen, B.R. Brooks, G.B. Fitzgerald, D.J. Fox, J.F. Gaw, N.C. Handy, W.D. Laidig, T.J. Lee, R.M. Pitzer, J.E. Rice, P. Saxe, A.C. Scheiner, H.F. Schaefer, PSI 2.0.8, PSITECH, Inc., Watkinsville, GA, 30677, USA, 1994.
[44] K.P. Huber, G. Herzberg, Constants of Diatomic Molecules, Van Nostrand Reinhold, New York, 1979.
[45] L. Pauling, The Nature of the Chemical Bond, 3rd ed., Cornell University Press, NY, 1960.
[46] R.M. Badger, J. Chem. Phys. 2 (1934) 128.
[47] R.M. Badger, J. Chem. Phys. 3 (1935) 710.
[48] Y. Yamaguchi, H.F. Schaefer, unpublished results.
[49] W. Kutzelnigg, Angew. Chem., Int. Ed. Engl. 22 (1984) 272.
[50] W. Kutzelnigg, J. Mol. Struct. 169 (1988) 403.